Title: Loss of control of epithelial basal extrusion leads to tumor resistance in *Drosophila*

Authors: M. Vialat[1,2]†, E. Baabdaty[1,2], C. Vachias[1,2], F. Degoul[1,2], A. Trousson[1,2], P. Pouchin[1], JMA. Lobaccaro[1,2], S. Baron[1,2], L. Morel[1,2], C. de Joussineau[1,2]*.

Affiliations:

[1]Université Clermont Auvergne, CNRS 6293, INSERM 1103, iGReD; Clermont–Ferrand, France.

[2] Groupe Cancer Clermont Auvergne; Clermont-Ferrand, France.

*Corresponding author. Email: cyrille.de_joussineau@uca.fr.

†Present address: Icahn School of Medicine at Mount Sinai, New York city, USA.

Abstract: Basal extrusion allows an epithelial cell to leave its compartment, making it a necessary step in the local invasion of all epithelial cancers. Here, we determined which effect sex steroid deprivation plays on basal extrusion, and the resulting consequences on tumorigenesis. For this, we blocked ecdysone signaling in a model of epithelial tumorigenesis in the drosophila accessory gland, in a tumor-cell specific manner. As for human treatment, this induces apoptosis of many preexistent tumor cells. It also slightly decreases primary tumor formation. However, it leads to the appearance of a new population of highly proliferative tumor cells following the loss of control of a newly discovered step of basal extrusion. Our findings suggest that steroid deprivation actively induces resistance by diverting highly controlled basal extrusion.

Introduction

National Cancer Institute defines cancer by their abnormal cells dividing without control and invading nearby tissues. Epithelial cancers represent around 90% of all cancers (Bray *et al*, 2018). As epithelial cells lie on a strong extracellular matrix on their basal side, epithelial tumor cells must cross this basement membrane to invade nearby tissues. For this reason, this step of invasion is called basal extrusion. Little is known about basal extrusion when it occurs physiologically during the development, but also when it occurs in the pathophysiological context of tumorigenesis. Basal extrusion still appears as a complex mechanism: it can be induced by the clonal expression of different oncogenes (Anton *et al*, 2018; Rambur *et al*, 2020; Villeneuve *et al*, 2019), may occur in balance with apical extrusion (Anton *et al*, 2018; Ventrella *et al*, 2023; Marshall *et al*, 2011), depends on multiple signaling such as the Notch (Ventrella *et al*, 2023), Ras/MAPK and PI3K/Akt pathways (Rambur *et al*, 2020) or PKC activation (Villeneuve *et al*, 2019). It depends on cholesterol uptake (Vialat *et al*, 2024) and lipid raft activity (Kajiwara *et al*, 2022), and can be promoted by extracellular matrix degradation even though it does not seem, counterintuitively, to be a necessary step (Shen *et al*, 2014). It also depends on a profound remodeling of cytoskeletal organization, cell-cell and cell-matrix interactions (Villeneuve *et al*, 2019; Ganier *et al*, 2018; Melo *et al*, 2023; Chountala *et al*, 2012; Slattum *et al*, 2009).

It is not known whether basal extrusion could also influence late progression of tumors towards resistance to therapies or metastatic stages, and then we tested this possibility. To do so, we used a previously published model of epithelial tumorigenesis in the accessory gland of drosophila (Rambur *et al*, 2020; Vialat *et al*, 2024). This gland being a functional equivalent of the prostate (Xue & Noll, 2002; Leiblich *et al*, 2012; Wilson *et al*, 2017), we selected resistance to sex steroid deprivation as the readout for our evaluation. Indeed, this resistance is associated to progression in prostate (Wu *et al*, 1994) but also in sex-steroid-dependent breast cancer (Clarke *et al*, 1989). So, our main strategy was to block drosophila sex steroid Ecdysone Signaling (Sharma *et al*, 2017; Sekar *et al*, 2023) in a tumorigenic context, to describe the impact on basal extrusion and the outcome of tumorigenesis, and to understand the molecular mechanisms leading to the main pathophysiologic modifications.

Results

Differential tumor resistance induced by loss of Ecdysone Signaling

In order to induce tumor-dependent basal extrusion, clonal expression of a constitutively active form of EGFR -EGFRλ- is realized in around 1% of main cells of the accessory gland (Rambur *et al*, 2020; Vialat *et al*, 2024). This oncogene is expressed with GFP, allowing tracing of tumor cells, and co-expressed with either nuclear GFP or RNAi against white, coding for an eye pigment, to provide an adequate control tumorigenesis (EGFRλ CTL). In these conditions, tumor cells can either stay inside the epithelium (Fig. 1A, white arrowheads) or develop into extra-epithelial tumors following basal extrusion (Fig. 1A, empty arrowheads), as shown by their

presence outside the muscle sheet that encloses the gland (revealed by F-actin staining in Fig. 1A and later). We previously showed that these extra-epithelial cells show phenotypic abnormalities typically associated to tumor development such as hyperplasia, hypertrophy, loss of expression of epithelial markers (visible here with the loss of expression of Fasciclin III in Fig. 1A) and promotion of angiogenesis-like tracheogenesis. We also previously showed that at least some of them retain one specific feature of accessory gland epithelial cells which is the presence of twin nuclei, confirming that these tumors are of accessory gland origin (Rambur *et al*, 2020).

Tumorigenesis divergence induced by loss of Ecdysone Signaling

Co-expression of an RNAi against Ecdysone Receptor EcR (EGFRλ EcR-KD), on the one hand, induces very similar epithelial clones and extra-epithelial tumors (Fig. 1B, left panels, white and empty arrowheads). On the other hand, it also induces appearance of a new kind of tumorigenesis, as large tumor masses now grow inside the glands (Fig. 1B, right panels, yellow arrowheads). In human, tumor cell death is induced by sex steroid deprivation (Isaacs *et al*, 1994; Dowsett *et al*, 2006). 6 days after clone induction (6D), cleaved-caspase 3 staining reveals that tumor cells in the control condition do not present signs of apoptosis (Fig. 1C, Fig. 1E, left column). At the same induction time, co-expression of EcR RNAi significantly induces apoptosis (Fig. 1D, empty arrowheads in left panels, Fig. 1E). At 10 days after induction (10D), most of the extra-epithelial tumors show apoptotic staining, independently of the phenotype (Fig.1d, empty arrowheads in right panels, Fig. 1E). Despite their ability to undergo basal extrusion, these cells seem unable to survive outside the glands. This is reminiscent of extracellular matrix detachment-induced apoptosis, or anoikis. On the contrary, with EcR downregulation, the new tumor cell population that grow inside the gland, in contact with the basement membrane, show no sign of apoptosis. Furthermore, they tend to invade the gland over time (Fig. 1D, yellow arrowheads in right panels), showing an uncontrolled and continuous proliferation. Together, this indicates that not only these cells are resistant to ecdysone deprivation, but also they now strive over time.

Tumor aggressiveness induced by loss of Ecdysone Signaling

Considering their hyperproliferative state, and so contrary to tumor cells in EGFRλ CTL condition, this new cell population logically displays strong staining for Ser10 Phospho-Histone 3 antibody (pH3), a marker of late phases of cell cycle prior to cell division (compare white to yellow arrowheads in Fig. 1F, upper panels). Furthermore, they exhibit a positive staining for a phosphorylated form of the proto-oncogene tyrosine-protein kinase Src (pSrc), a classical marker of aggressiveness (Fig. 1F, lower panels) (Baumgartner *et al*, 2008). These tumor cells also display many typical defects, such as a clear pleomorphism with either compact or fusiform cells, and strongly disorganized clones (Fig. 1G). In the same clones and even in the same cell, cell nuclei display strong difference in size (anisocaryosis) with frequent hypertrophied nuclei (macrocaryosis) (see for example cells in the top left panel in Fig. 1G). Number of nuclei itself can be abnormal (empty arrowheads showing a trinucleated cell, top left panel in Fig. 1G), and nuclei forms are frequently altered (empty arrowheads in lower panels in Fig. 1G). Also, clones can grow along multiple axes (double-headed arrowheads in top right panel in Fig. 1G) and

present a strong fibrillar framework (zoom in same panel). Together, these results highlight that this new population has reached a more aggressive step of tumor progression, compared to previously described clones but also to previously described extra-epithelial tumors which, despite their loss of epithelial markers, display rounder shapes and form well-delimited tumors.

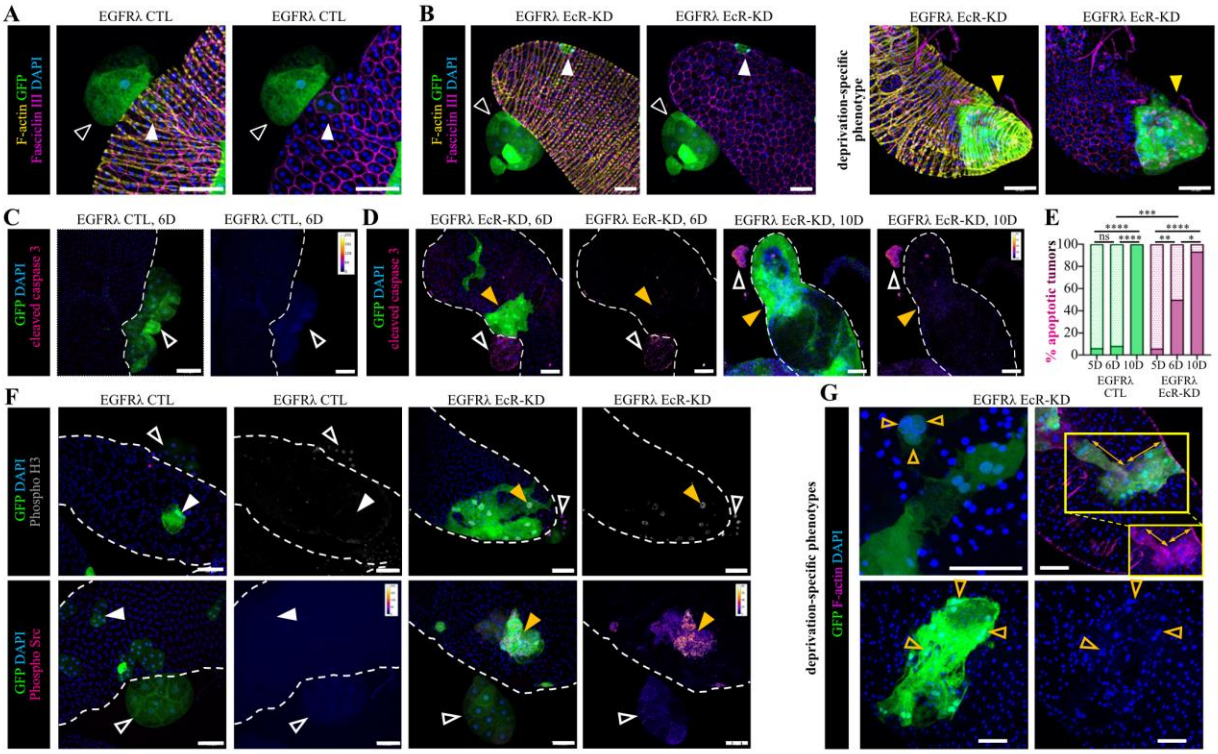

Fig. 1. Down-regulation of Ecdysone Signaling induces both apoptosis and aggressiveness in tumor cells. (**A**) Clonal expression of EGFRλ oncogene induces two phenotypes: overgrowth of epithelial cells (white arrowheads) and formation of extra-epithelial tumors consecutively to basal extrusion (empty arrowheads). (**B**) Co-expression of EcR RNAi leads to the same phenotypes (left panels) but also to the appearance of a "deprivation-specific" phenotype where large clones of tumor cells appear in the glands (right panels, yellow arrowheads). (**C**) At 6 days of induction (6D), extra-epithelial tumors do not normally accumulate cleaved-caspase 3 apoptotic marker. (**D**) Co-expression of EcR RNAi induces accumulation of the same apoptotic marker in the extra-epithelial tumors from 6 days of induction (left panels) but not in the new tumor cell population (yellow arrowheads) that invades the gland over time (right panels, at 10 days of induction). (**E**) Quantification of cleaved-caspase 3 stained extra-epithelial tumors over time. (**F**) Compared to the other tumor cells and independently of genotype, the new tumor cell population accumulates high levels of proliferation (Phospho-Histone 3, upper panels) and aggressiveness (Phospho-Src, lower panels) markers. (**G**) The new tumor cell population accumulates morphological defects associated to aggressiveness. Scale bars: 50µm. Number of experiments and of individual flies given in Table S1.

Control of two-step basal extrusion by ecdysone signaling

The two steps of basal extrusion revealed by loss of Ecdysone Signaling

In EGFRλ CTL condition (Fig. 2A, white arrowheads in left panels) as in case of co-repression of Ras/MAPK, PI3K/Akt (Rambur *et al*, 2020) or cholesterol metabolic pathway (Vialat *et al*, 2024), tumor clones in the gland remain strictly in the epithelium. On the contrary, in EGFRλ EcR-KD condition, when expanding in the gland, the new population of tumor cells grow between normal epithelium and basement membrane (Fig. 2B, yellow arrowheads in right panels). So, these cells were able to basally migrate out of the normal epithelium, but either failed or somehow chose not to cross the basement membrane. This shows that basal extrusion is in fact a two-step phenomenon: in the first step, cells leave the epithelium, and in the second, independent step, they can cross the basement membrane and leave the epithelial compartment. In EGFRλ CTL condition, these two steps are efficiently coupled, and so appear as a single phenomenon. However, the second step seems under the control of Ecdysone Signaling; so, when this pathway is impaired, part of the tumor cells only undergo the first step and then grow between the normal epithelium and the basement membrane, in what we define as the intrabasal (IB) compartment, creating intrabasal tumors.

Moderate inhibition of basal extrusion by loss of Ecdysone Signaling

This suggests that loss of Ecdysone Signaling should decrease extra-epithelial tumor growth. However, at 6D, tridimensional reconstruction show that these tumors display the same volume and same number of cells as in EGFRλ CTL condition (Fig. 2C). They so display the same proliferation rate of around 700% (Fig. 2C), compared to clones expressing GFP only, which are composed of 2 cells at 6 days of induction (example in Fig. S3A). Furthermore, temporal dynamics of extra-epithelial tumor formation is not affected by co-expression of EcR RNAi (Fig. 2D): extra-epithelial tumors typically appear during the third and fourth days after clonal induction to peak at 5D regardless of tested genotypes, indicating that basal extrusion is active only during this short-time period. However, a modest but significant decrease in the total extra-epithelial tumor formation is detected in case of EcR downregulation (Fig. 2E). Together, these data show that loss of Ecdysone Signaling specifically affects the global quantity of tumor basal extrusion, but has neither an effect on its temporal dynamics of formation nor on the tumor growth rate outside the gland.

Prolonged activation of intrabasal tumorigenesis by loss of Ecdysone Signaling

At 6D, intrabasal tumors (IB-T) are significantly smaller than extra-epithelial tumors (T) but still significantly larger than epithelial clones of EGFRλ CTL genotype (C) (Fig. 2F). This increase in volume mostly comes from an increased proliferation rate and so an increased tumor cell number in these intrabasal tumors, that at 6D already compare with those of extra-epithelial tumors (Fig. 2F). Furthermore, contrary to extra-epithelial tumors, intrabasal tumors continue to appear and grow over time, as more glands display at least one intrabasal tumor at 7D than at 6D (Fig. 2G). So, even though loss of Ecdysone Signaling slightly decreases full basal extrusion and accelerates apoptosis of extra-glandular tumors, it overall strongly increases the proliferation and

progression (Fig. 1F-G) by inducing the growth of resistant tumors into the intrabasal compartment.

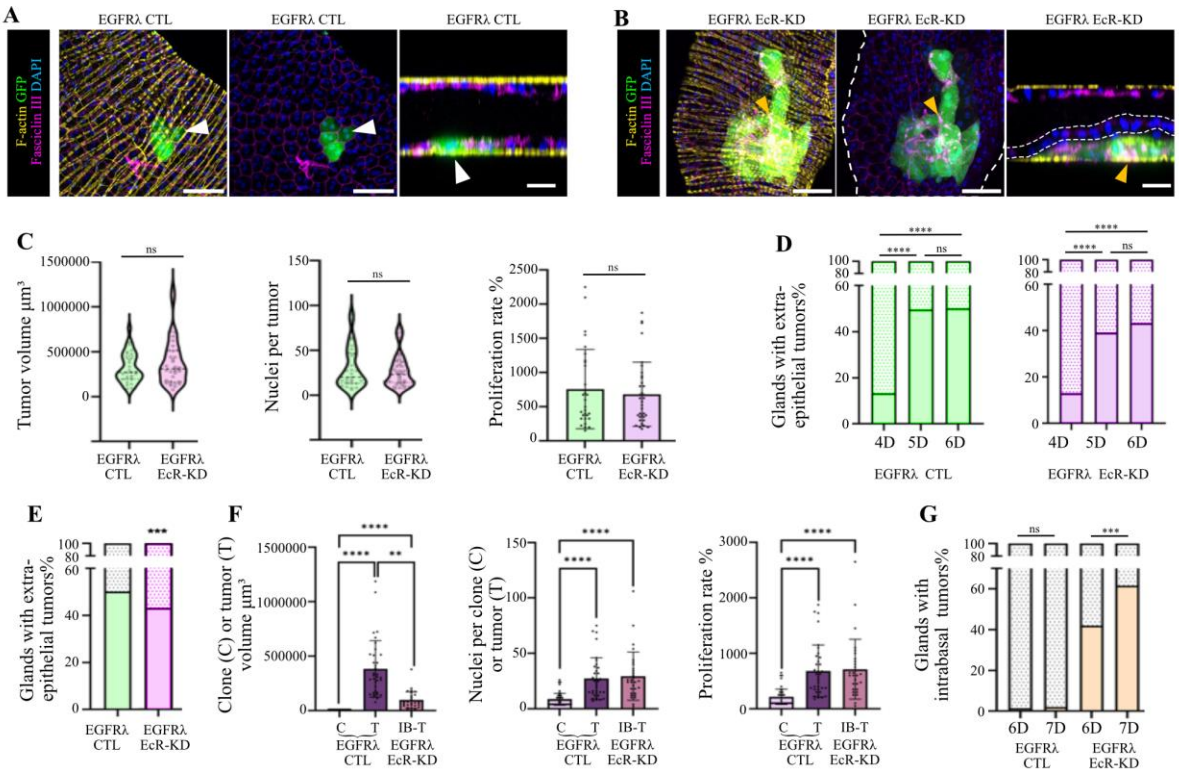

Fig. 2. Down-regulation of Ecdysone Signaling reveals a two-steps, two-tumor cell fates basal extrusion. (**A**) In EGFRλ CTL flies, intra-glandular clones (left panels) are strictly epithelial (XZY right panel). (**B**) In case of EcR RNAi co-expression, the large clones of tumor cells now grow between the normal epithelium (dotted lines) and the basement membrane (XZY right panel, yellow arrowhead), in a new intrabasal compartment. (**C**) Extra-epithelial tumor features are not affected by down-regulation of Ecdysone Signaling. (**D**) Extra-epithelial tumors all appear within five days of clonal induction independently of the genotype. (**E**) EcR RNAi co-expression significantly decreases extra-epithelial tumor formation. (**F**) 6 days after induction, intrabasal tumors display significantly higher proliferation than epithelial clones of EGFRλ CTL condition. (**G**) Contrary to extra-epithelial tumors, intrabasal tumors grow specifically in EGFRλ EcR-KD condition and continue to appear over time. Scale bars: 50µm, or 20µm in right panel in A and B. Number of experiments and of individual flies given in Table S1.

Ecdysone-dependent molecular control of basal extrusion

Resistance to androgen deprivation is generally considered as an ability for AR to activate its target genes despite the hormone deprivation and/or to play through activation of non-genomic

pathways. As our primary strategy was to decrease EcR (Fig. S1), this is important to understand whether the observed resistance results from a mechanism of escape or from a real lack of Ecdysone Signaling. To understand the exact role of Ecdysone Signaling in intrabasal tumor appearance, we then downregulated multiple targets at different levels of this pathway (Fig. S2). We also tested the effect of a loss of Ecdysone Signaling in a normal context. We found that, by itself, this loss does not induce tumorigenesis by itself (Fig. S3D): at 6D, clones are composed of two cells (Fig. S3B-C), as for expression of GFP only (Fig. S3A), showing no abnormal proliferation, and the cells appear of normal shape and nuclei number (Compare Fig. S3B and S3C to S3A). The only detected phenotype is a slight decrease in epithelial cell growth, which was expected from ecdysone role in accessory gland cell differentiation: this decreased growth probably reflects a partial loss in their ability to produce seminal fluid (Fig. S3F). We then decreased with different approaches Ecdysone Signaling in a tumoral context.

Lack of canonical Ecdysone Signaling drives tumor resistance

Paralleling human metabolization of testosterone into active DiHydroTestosterone (DHT) by SRD5A2 gene product, ecdysone must be metabolized into active 20-hydroxyecdysone by Shade (Shd) (Petryk *et al*, 2003). Tumor progression in glands of EGFRλ Shd-KD phenocopies the one in EGFRλ EcR-KD condition, both for the decrease in extra-epithelial tumors and the appearance and growth of resistant intrabasal tumors (Fig. 3A, magenta columns). By targeting an independent gene, this confirms that this is the lack of EcR signaling that leads to resistance in the drosophila accessory gland. Furthermore, Ecdysone Signaling relies on the recruitment of specific EcR target genes, the early-late transcription factors Hr3 and Hr4, to drive ecdysone response (Carney *et al*, 1997; Gauhar *et al*, 2009). Once more, tumor progression in both EGFRλ Hr3-KD and EGFRλ Hr4-KD conditions are strikingly similar to EGFRλ EcR-KD condition (Fig. 3A, blue columns, Fig. 3B, Fig. S4), showing that this is the lack of canonical Ecdysone Signaling that leads to resistance.

Complete dependence on tumor-produced Ecdysone

Prostate cancer cells are able to produce steroids (Locke *et al*, 2008) which participate to AR reactivation in castration-resistant prostate cancer (CRPC) (Cai *et al*, 2011). In drosophila, Halloween genes encode the enzymes that synthetize ecdysone. Phantom (Phm) is the limiting enzyme catalyzing the antepenultimate step, and Shadow (Sad) is the terminal enzyme. EGFRλ Phm-KD and EGFRλ Sad-KD conditions again phenocopy EGFRλ EcR-KD condition (Fig. 3A, red columns, Fig. 3B, Fig. S5). This shows by targeting still two other independent genes and another process that, in the drosophila accessory gland, growth of intrabasal resistant tumors results from a lack of Ecdysone Signaling. Furthermore, this also demonstrates that circulating ecdysone is unable to compensate for the lack of tumor-produced ecdysone, which represents then the only dispensable resource to sustain tumorigenesis in EGFRλ CTL condition. We previously demonstrated that autocrine loops recruiting Ras/MAPK and PI3K/Akt pathways are established to support basal extrusion (Rambur *et al*, 2020). We show here that there is also establishment of an autocrine/intracrine loop to activate Ecdysone Signaling and sustain the same

phenomenon. However, blocking this loop now induces growth of intrabasal resistant tumors, contrary to inhibition of Ras/MAPK and PI3K/Akt pathways.

EcR targets implicated in the two steps of basal extrusion

We then searched for molecular control of the two steps of basal extrusion. We previously showed that drosophila *Insulin-like peptide 6* (*Ilp6)* is specifically overexpressed during accessory gland tumorigenesis and participates to basal extrusion (see also Fig. 3C), but is not associated to intrabasal tumor growth (Rambur *et al*, 2020). Ilp6 is a target of EcR signaling (Slaidina *et al*, 2009). In the accessory gland, both EGFRλ EcR-KD or EGFRλ Sad-KD conditions show significantly decreased Ilp6 expression levels (Fig. 3C), which can explain the lower formation of extra-epithelial tumors in these conditions.

We then screened for potential actors of intrabasal growth. Cytoskeletal reorganization is a major determinant of tumor cell invasion and resistance, and intrabasal tumor cells show profound cytoskeletal reorganization. *Beta Tubulin at 60D* (*Tub60D*) encodes for β3 Tubulin and is a target or Ecdysone Signaling (Bruhat *et al*, 1990). β3 Tubulin accumulates in intra-epithelial clones of EGFRλ CTL condition but is mostly absent in intrabasal tumor cells (Fig. 3D). Down-regulation of Tub60D (EGFRλ Tub60D-KD condition) is sufficient to induce intrabasal growth (Fig. 3E and Fig. 3F, right columns), but has overall no effect on the formation of extra-epithelial tumors (Fig. 3F, left columns). Furthermore, these extra-glandular tumors in this condition are still unchanged compared to the other tested conditions (Fig. S6), showing that it is only the intrabasal growth which is favored by this downregulation of Tub60D. More interestingly, in this case, the tumor cells that grow in the intrabasal compartment does not proliferate more than epithelial clones (Fig. 3G). So, lack of β3 Tubulin appears as a major determinant of intrabasal growth but does not seem to promote aggressiveness by itself.

Expression profiles in human prostate cancer

Collections of the most comprehensive cohorts were recently pooled by Bolis et al (Bolis *et al*, 2021), allowing to revisit the molecular mechanisms associated to prostate cancer progression thanks to the prostatecanceratlas.org interface. Along with cancer progression (pseudotime correlation in Fig. 3H), AR expression very slightly increases. However, AR signaling appears as the most repressed pathway along with cancer progression (Bolis *et al*, 2021), and expression of its canonical target genes, such as *KLK3*, largely decreases in the most advanced CRPC tissues (Fig. 3H). Interestingly, one the most repressed gene along with prostate cancer progression is *SRD5A2* (Fig. 3H), which could limit metabolization of DHT, the active form of Testosterone, and so participate also in the decrease of AR signaling during progression. *IGF1* and *TUBB6* are among the orthologs of *Ilp6* and *Tub60D*. As AR signaling decreases with prostate cancer progression, *IGF1* and *TUBB6* expression also steadily decreases (Fig. 3H). As *TUBB6* lack of expression has been associated to treatment resistance and progression of epithelial cancers (Nami & Wang, 2018; Leandro-García *et al*, 2010), it could participate to prostate cancer progression also.

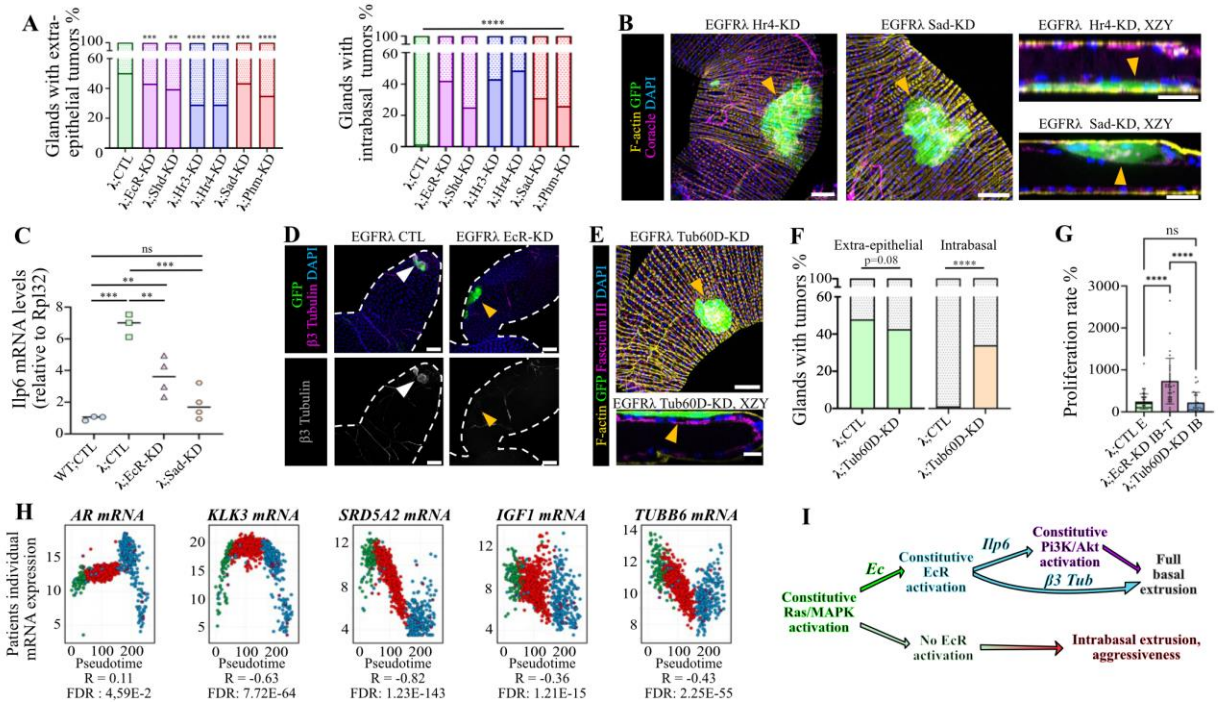

Fig. 3. Molecular control of the two-step basal extrusion by Ecdysone signaling. (**A**) Down-regulating early-late response genes (blue) of canonical EcR response or intra-tumoral ecdysone synthesis (red) induces the same reduction in extra-epithelial tumors formation and the same growth of intrabasal tumors. (**B**) Representative images of intrabasal tumors (yellow arrowheads) for two genotypes. (**C**) Down-regulation of Ecdysone Signaling impairs the EGFRλ-induced Ilp6 overexpression. (**D**) Down-regulation of Ecdysone Signaling impairs the EGFRλ-induced Tub60D overexpression. (**E**) Down-regulation of Tub60D is sufficient to induce intrabasal growth in EGFRλ-expressing cells. (**F**) Down-regulation of Tub60D does not affect formation of extra-epithelial tumors but promotes consistent intrabasal growth. (**G**) In EGFRλ Tub60D-KD flies, intrabasal cells do not proliferate more than epithelial cells of EGFRλ CTL flies. (**H**) During prostate cancer progression, despite slight increase in AR expression, AR signaling significantly decreases along with orthologs of Ilp6 and Tub60D. (**I**) Ecdysone deprivation induces an alternative tumor fate. Scale bars: 50µm, or 20µm in right panel in B and 10µm in lower panel in E. Number of experiments/cohorts and of individual flies/patients given in Table S1.

Discussion

Overall, basal extrusion of tumor cells appears as a two-step phenomenon which is tightly regulated by Ecdysone Signaling, and down-regulation of this signaling induces growth of aggressive intrabasal tumors (Fig. 3I). This circumvents anoikis that is still accelerated by ecdysone deprivation (Fig. 1E) and allows a massive spreading of hyperproliferative tumor cells at the interface between normal epithelial cells and the basement membrane. Interestingly, clonal expression of an oncogene in mice epithelia induces the formation of dome-like structures where

tumor cells accumulate at the same localization (Shirai *et al*, 2022). This localization has been known for decades to favor tumor growth, as exemplified by the widespread use of subcapsular renal xenografting in the field of cancer research (Bogden *et al*, 1979). Moreover, in a mouse model of intraductal human breast carcinogenesis, Zoeller et al have demonstrated that tumor cells adjacent to basement membrane display extra-resistance to treatments when compared to others, indicating that this specific microenvironment is most adapted for cell survival upon treatment (Zoeller *et al*, 2017).

However, we were able to push tumor cell growth in this compartment by playing on Tub60D expression (Fig. 3E-F). In that case, no increase in cell proliferation (Fig. 3G), no apparent cell disorganization (Fig. 3E) are associated to this intrabasal growth. So, by itself, the fact that cells grow into the intrabasal compartment is not sufficient for tumor progression. At the opposite, in the drosophila accessory gland, tumor cell resistance is acquired by a decrease in Ecdysone Signaling. This is reminiscent of breast cancer, where loss of ER is a common event largely associated to tumor aggressiveness (Kuukasjärvi *et al*, 1996), and of prostate cancer, where, despite common wisdom, many of the AR mutations found in tumors are loss of function (Hay & McEwan, 2012). Moreover, in human, Androgen Deprivation Therapy (ADT) shows opposite effects depending on the cancer stage. For poorly differentiated tumors or metastatic stages, ADT has largely proven its efficacy by increasing survival of patients. However, for localized prostate cancer, some studies argue that ADT displays no beneficial effect and is even associated with worse outcome than active surveillance for patients survival (Merglen *et al*, 2007; Lu-Yao *et al*, 2008). Besides, for men suffering from hypogonadism, testosterone supplementation therapy has been feared to increase the risk of prostate cancer. However, reviews of the scientific literature show strictly no increase in the incidence of this treatment on prostate cancer (Michaud *et al*, 2015; Dupree *et al*, 2014). Finally, in High-Grade Prostate Intraepithelial Neoplasia (HGPIN), this is low testosterone that is correlated to an increased risk of prostate cancer development (García-Cruz *et al*, 2012).This suggests that a decreased activity of sex steroid signaling in the early phases of tumorigenesis could be implicated in cancer progression and/or the genesis of population of tumor cells that are resistant to endocrine therapy.

So, overall, we show that, *in vivo*, epithelial basal extrusion is a two-step phenomenon. We show that repression of sex steroid signaling in an oncogenic context induces a specific change of tumor cell fate, where these cells now grow in a newly unveiled intrabasal compartment. We show that, for tumor cells, this represents a key event in their progression and in the genesis of resistance to sex steroid deprivation. Epithelial basal extrusion, which remains an elusive event, could then be a major source of tumor aggressiveness, depending on the modulation of activity of specific pathways such as sex steroid signaling.

Materials and Methods

Fly stocks and experimental crosses

y,w,HS:flp122/+;Act:FRTstopFRTGal4, UAS:GFP/CyO flies allowed conditional clonal expression of GFP. Combination with UAS:EgfrλTop (#59843) allowed conditional clonal co-

expression of GFP and Egfrλtop (EGFRλ flies). EGFRλ flies were then crossed with following stocks to realize experiments: UAS-GFP.nls or RNAi White (#4775 or #33623, control condition), UAS-EcR RNAi (#50712), UAS-Shd RNAi (#67456), UAS-Hr3 RNAi (#27253), UAS-Hr4 RNAi (#54803), UAS-Sad RNAi (#67352), UAS-Phm RNAi (#65017), UAS-Tub60D RNAi (#64856) from the Bloomington Stock Center.

Conditional expression induction

Briefly, flippase (flp)/FRT system was activated by a 12 min heat-shock induction at 37°C during the pupal stage, to create an average of 4–6 clones per accessory gland (≈1% of total number of epithelial cells). Flies were then kept at 27 °C until the end of pupal stage. Males were collected at emergence from pupae 3 to 3.5 days after heat shock and kept for another 1 to 5 days at 27 °C before dissection.

Immunohistochemistry and imaging

Accessory glands were dissected in PBS, fixed for 10 min in 4% paraformaldehyde, washed and permeabilized for 15 min in PBS containing 0.2% Triton (PBS-T). Glands were blocked for one hour with 0.5% of BSA in PBS-T then incubated overnight at 4°C with primary antibodies diluted in the same blocking solution. After three washes in PBS-T, glands were incubated in secondary antibody diluted 1:1000 in blocking solution for 1 hour at room temperature with DAPI (DiAminidoPhenylIndol, D8417, Sigma) 1:1000 (DNA staining) and/or Alexa633-phalloidin (A22284, Life Technology) 1:5000 (to reveal F-actin). Glands were then washed twice in PBS-T, once in PBS and subsequently mounted in Vectashield (#-1000, Vector Laboratories). Imaging was realized on Leica SP8 confocal microscope, and image stacks were processed either in ImageJ or Imaris software. All stainings were repeated a minimum of 3 times on independent experiments.

List of antibodies: Mouse Coracle (1:300, #C566.9 DSHB), mouse Fasciclin III (1:400, #7610 DSHB), goat GFP (1:1000, #5450 Abcam), rabbit pSrc (1:500, #44-660G Invitrogen), rabbit pH3 (1:500, #06-570, Merck Millipore), rabbit cleaved-caspase 3 (1:400, #9661S, Cell Signaling), secondary antibodies coupled to different fluorophores 488 (1:1000, A11055 Invitrogen), Cy3 or Cy5 (1:1000, 711-165-152, 715-165-151, 715-175-150, Jackson Immunology).

Clones sizes, cells and nuclei size and numbers, proliferation rate

Clones/tumors sizes, cells and nuclei volumes and numbers were determined from 3D reconstruction and automatic quantification in Imaris software. For each clone/tumor, average cell size was determined by ratio between clone size and number of nuclei in the considered clone. Proliferation rate was calculated compared to number of cells in a clone expressing GFP only (as in Fig. S3A). A typical clone is composed of 2 cells, and so 2 cells was taken as 100% proliferation. See table S1 for the number of experiments and total numbers of individual flies that were processed for each experiment.

Invasive tumor frequency

Tumor frequency was determined as the percentage of flies that displayed at least one tumor on their accessory glands at dissection. See table S1 for the number of experiments and total numbers of individual flies that were processed for each experiment.

RNA extraction, cDNA synthesis and Real-Time Quantitative PCR

RNAs were extracted from accessory glands dissection, by Trizol-extracted total accessory glands (InVitrogen). Reverse transcription was performed using SuperScript IV Reverse Transcriptase kit (ThermoFischer Scientific). Quantitative PCR was performed using the LC480. Rpl32 was used for the normalization.

Primers for qRT-PCR analysis

Rpl32: forward: 5′-TTGGCTTCGGTTTCCGGCAAG-3′; reverse: 5′-ATCGA TCCGACTGGTGGCGGAT3′; Dilp6: forward: 5′ TGCTAGTCCTGGCCACCTTGTTCG-3′; reverse: 5′ GGAAATACATCGCCAA GGGCCACC-3′; Spitz: forward: 5’ AATATTGGGCCTGGGCGTGG-3’; reverse: 5’ CCGCGCCTCTTCGATCTCCTC-3’; Sad: forward: 5′ CCGCATTCAGCAGTCAGTGG-3’; reverse: 5’ ACCTGCCGTGTACAAGGAGAG.

RNA FISH

Single-molecule RNA fluorescence in situ hybridization (smRNA-FISH) for transcripts of ECR from the accessory gland was performed using Stellaris probes (Biosearch Technologies). Probe sequences are listed in table S1. Accessory gland were dissected in PBS and fixed in 4% formaldehyde, 0.3% Triton X-100, 1x PBS for 20 min at room temperature, rinsed and permeabilized in 70% ethanol at 4°C overnight. Glands were rehydrated in smRNA FISH wash buffer (10% formamide in 2x SSC) for 10 min, resuspended in 50µL hybridization buffer (10% dextran sulphate, 10% formamide in 2xSSC) supplemented with 1.5µL of smRNA FISH probes. Hybridization was performed at 37°C overnight. Glands were then washed twice with smRNA FISH wash buffer at 37°C for 30 min and twice with 2xSSC solution. Then, DNA was stained with DAPI (1/500 dilution in 2x SSC) at room temperature for 20 min. Accessory glands were then mounted in 30µL Vectashield prior to imaging. The resulting images were processed using FIJI/ImageJ.

Statistical analyses and human data

All experiments were repeated independently a minimum of three times (N: number of independent experiments) on numerous glands (n: number of pairs of glands or number of imaged and quantified glands for tumor size and nuclei number quantification; see table S1). Statistical analyses were performed using GraphPad Prism 6 for tumor size and nuclei number quantification were compared by Krustal-Wallis test; % of glands with extra-glandular tumors were compared by Chi2 test; gene expression in qPCR was compared by two-tailed impaired T-test. In all figures, significance is described as follows : * $P < 0.05$; ** $P < 0.01$; *** $P < 0.001$; **** $P < 0.0001$. Human data processing was done using the tools developed by Bolis et al. and available at prostatecanceratlas.org.

Data and materials availability: All data are available in the main text or the supplementary materials.

Author contributions:

Conceptualization: MV, SB, LM, CJ

Methodology: MV, EB, EV, AT, PP, LM, CJ

Software: PP

Validation: MV, EB, CJ

Investigation: MV, EB, CJ

Visualization: MV, EB, LM, CJ

Funding acquisition: MV, JML, SB, LM, CJ

Project administration: LM, CJ

Supervision: MV, EB, LM, CJ

Writing – original draft: MV, EB, LM, CJ

Writing – review & editing: FD, JML, SB

Competing interests: Authors declare that they have no competing interests.

Acknowledgments: The authors thank N. Anglaret, L. Babkina, A. De Haze, C. Gaudichet and C. Tamisier for technical help; Dr E. Chautard and Dr A. Bruhat for scientific advices; Bloomington Drosophila Stock Center (BDSC) for providing fly stocks, and Drosophila Studies Hybridoma Bank (DSHB) for providing antibodies. Dr Krzysztof Jagla for kind gift of β3 tubulin antibody. CLermont Imagerie Confocale (CLIC) facility for support with imaging. La ligue contre le cancer (CJ), La Fondation ARC (MV), French Center for the 3Rs (FC3R) grant Re-Innov (CJ) for funding.

Supplementary Materials

Figs. S1 to S6, Table S1.

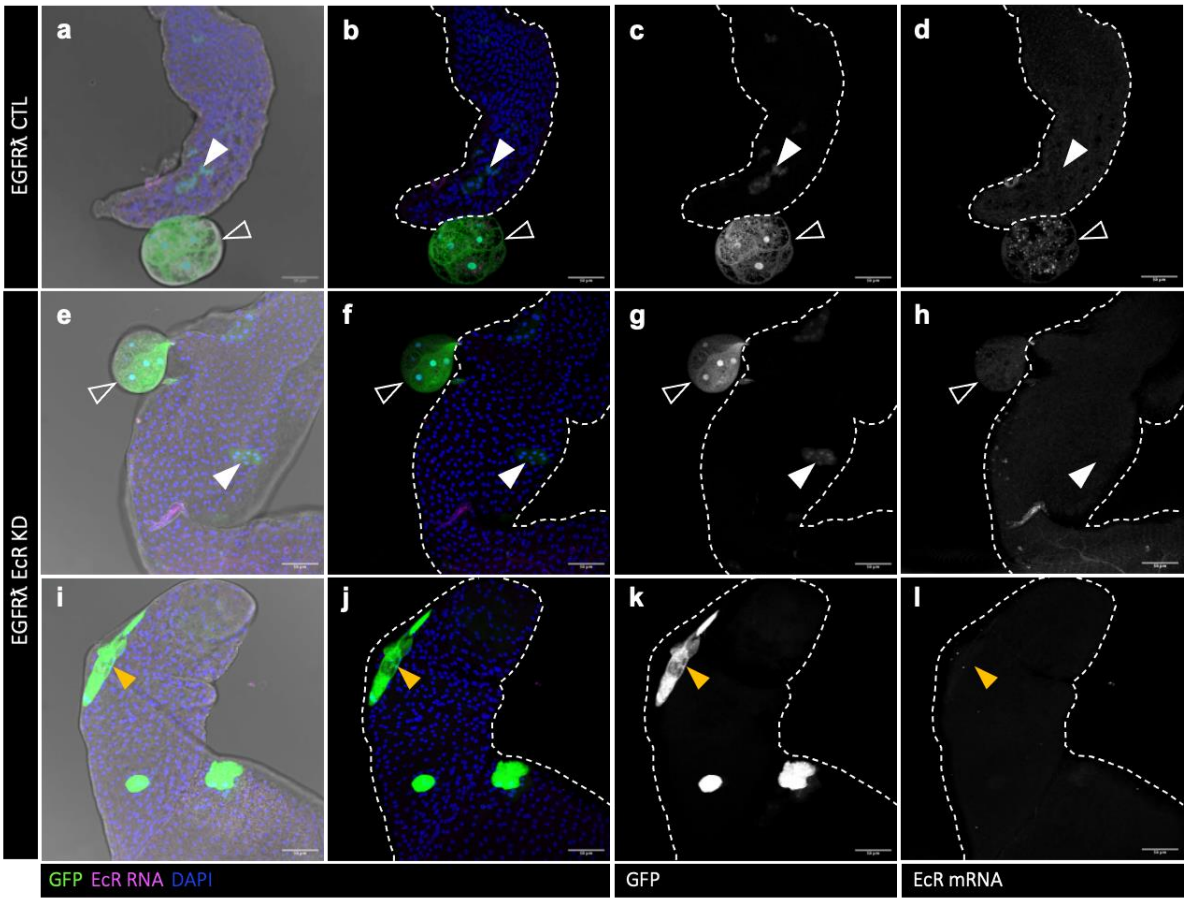

Figure S1: EcR RNAi efficiently downregulates EcR mRNA overexpression in tumor cells. (a-d) FISH staining reveals that EGFRλ clonal expression induces overexpression of EcR mRNA in tumor cells (empty arrowheads, EcR mRNA staining alone in (d)). (e-l) EcR RNAi co-expression efficiently downregulates EcR mRNA in tumor cells (empty arrowheads in (e-h)) as well as in intrabasal tumor cells (yellow arrowheads in (i-l)). Representative images from three or more experiments. Scale bars: 50 μM.

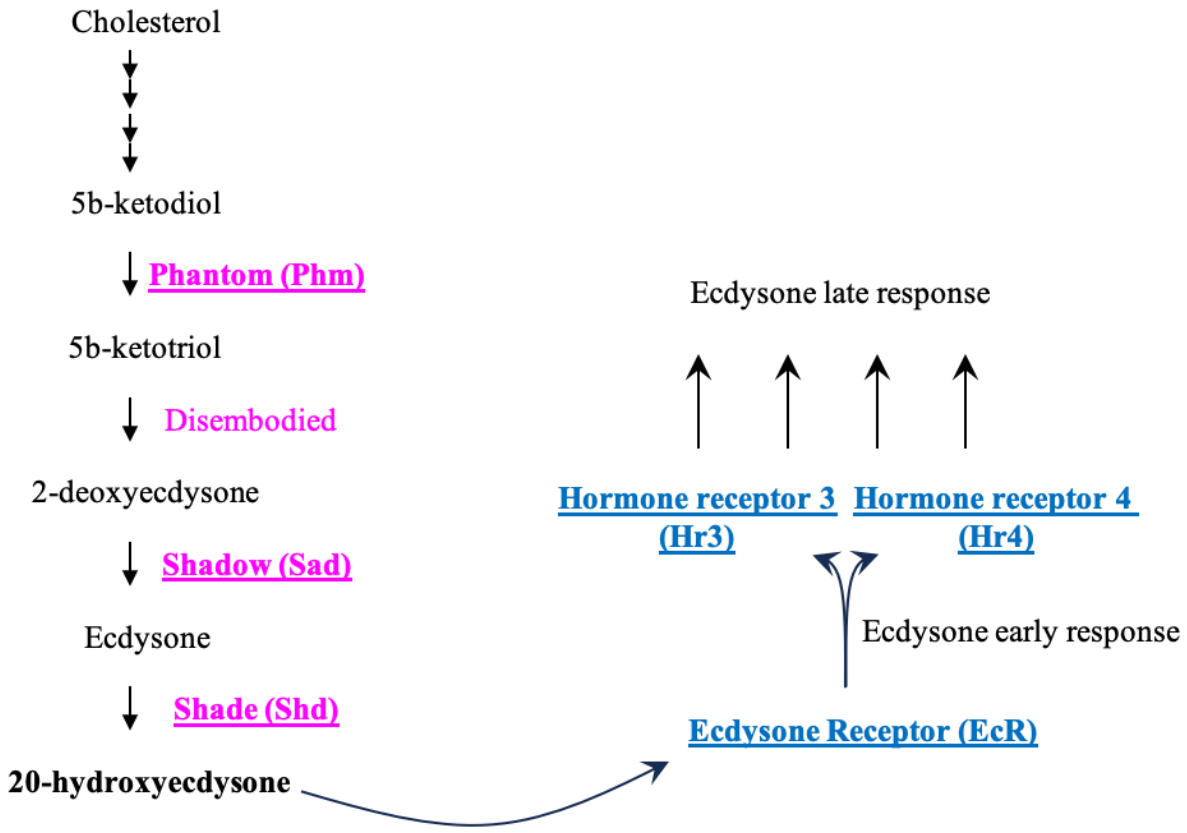

Figure S2: Schematic representation of late steps of ecdysone synthesis and canonical Ecdysone Signaling.

Six different genes (underlined) were independently targeted by RNAi to block tumor cell production of ecdysone (Phm, Sad), metabolization of active 20-hydroxyecdysone (Shd), or EcR Signaling (EcR, Hr3, Hr4). All of these experiments induced the same phenotypes, indicating that downregulation of canonical Ecdysone Signaling induces a diversion of basal extrusion, and that Ecdysone Signaling in tumor cells only relies on intra-tumoral ecdysone synthesis.

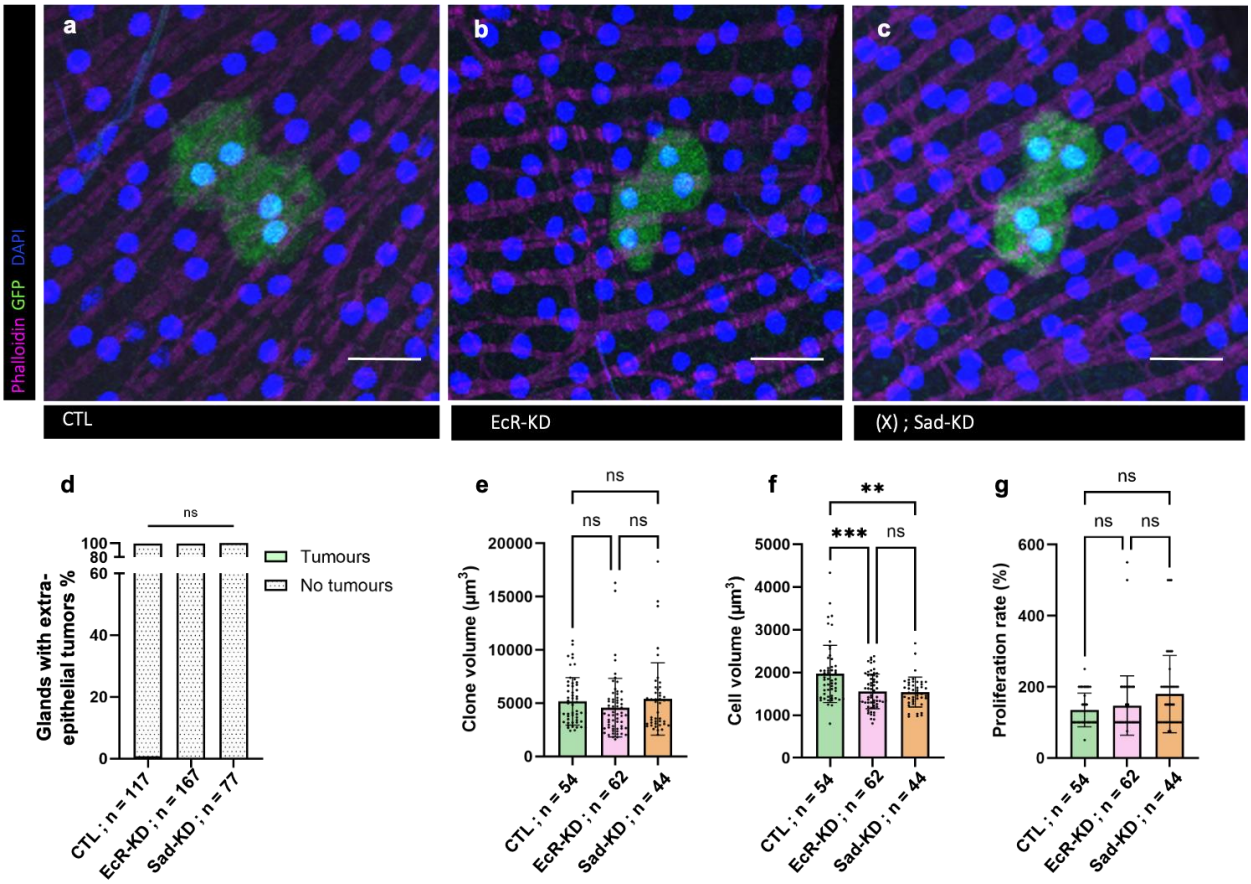

Figure S3 – Ecdysone deprivation does not promote tumorigenesis by itself.
(a-c) In the absence of expression of an oncogene (CTL), clonal induction of NLS-GFP (a) EcR RNAi (b) or Sad RNAi (c) brings no evident phenotype to the clonal cells. (d) It does not promote tumorigenesis. (e-g) In the absence of average clone volume (e) or proliferation rate compared to control (g), the only noticeable phenotype is a slight decrease in the size of cells expressing EcR or Sad RNAi (f). Chi^2 test; **P < 0.01; ***P < 0.001. Representative images in (a-c) from three or more experiments. Scale bars: 20 µm.

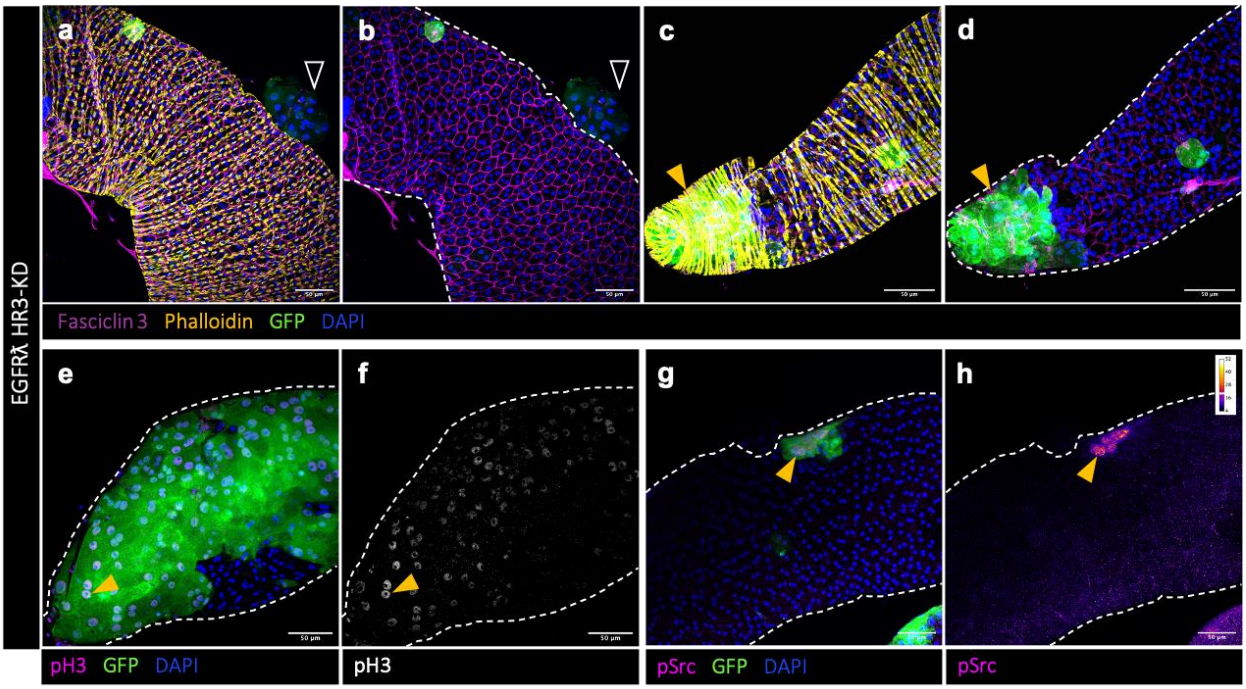

Figure S4 - Downregulation of canonical Ecdysone Signaling induces invasion and aggressiveness.

(a-d) Co-expression of Hr3 RNAi only partially suppresses extra-epithelial tumor formation (empty arrowheads in (a-b)) but also leads to the appearance of highly proliferative, resistant intrabasal tumor cells into the glands (yellow arrowheads in (c-d)). (e-h) This new population displays a strong staining for classical aggressiveness markers (yellow arrowheads, pH3 staining in (e-f) and pSrc staining in (g-h)). Representative images from three or more experiments. Scale bars: 50 μM.

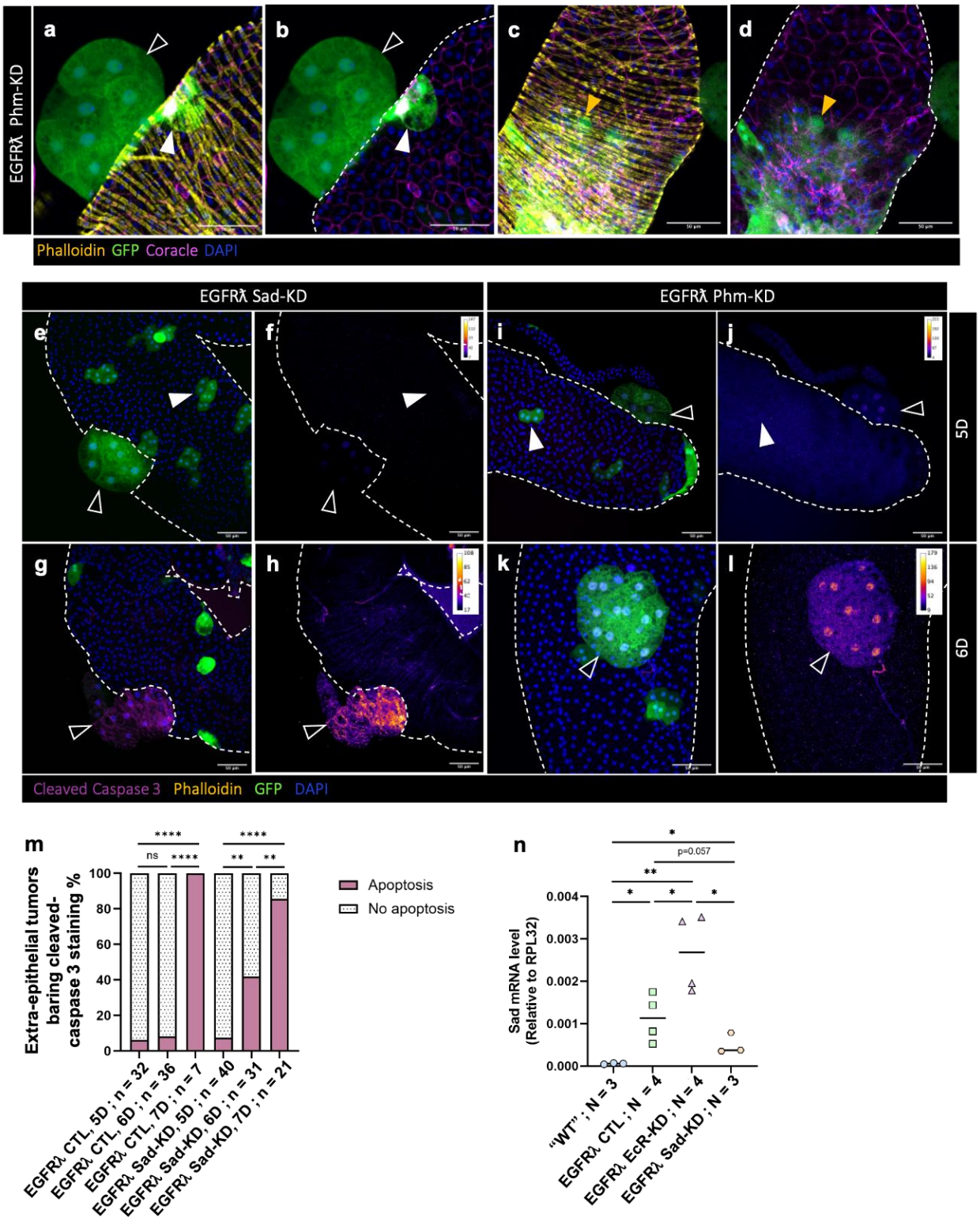

Figure S5 – Loss of autocrine Ecdysone Signaling induces same paradoxical response as loss of other members of the same pathway.

(a-d) Co-expression of Phm RNAi only partially suppresses the formation of extra-epithelial tumors (empty arrowheads in (a-b)) but also leads to the appearance of highly proliferative,

resistant intrabasal tumor cells (yellow arrowheads in (c-d)). (e-l) Co-expression of Sad (RNAi (e-h) or Phm RNAi (i-l) induces early apoptosis of extra-epithelial tumors (at 6D, cleaved-caspase 3 staining), mimicking initial effect of steroid deprivation on human tumors (empty arrowheads). (m) Quantification of this early apoptosis phenomenon appearing at 6D for the co-expression of Sad RNAi. (n) qPCR quantification of whole glands expression of Sad for the given genotypes. "WT": glands baring the EGFRλ genetic background, but unable to produce clones, i.e. "wild type" glands. Compared to these, oncogene induction (column 2) induces a significant overexpression of Sad mRNA; co-expression of EcR RNAi (column 3) still significantly increases Sad mRNA expression. Compared to this condition, co-expression of Sad RNAi (column 4) significantly decreases Sad mRNA expression, as expected. Representative images in (a-l) from three or more experiments. Scale bars: 50 μM.

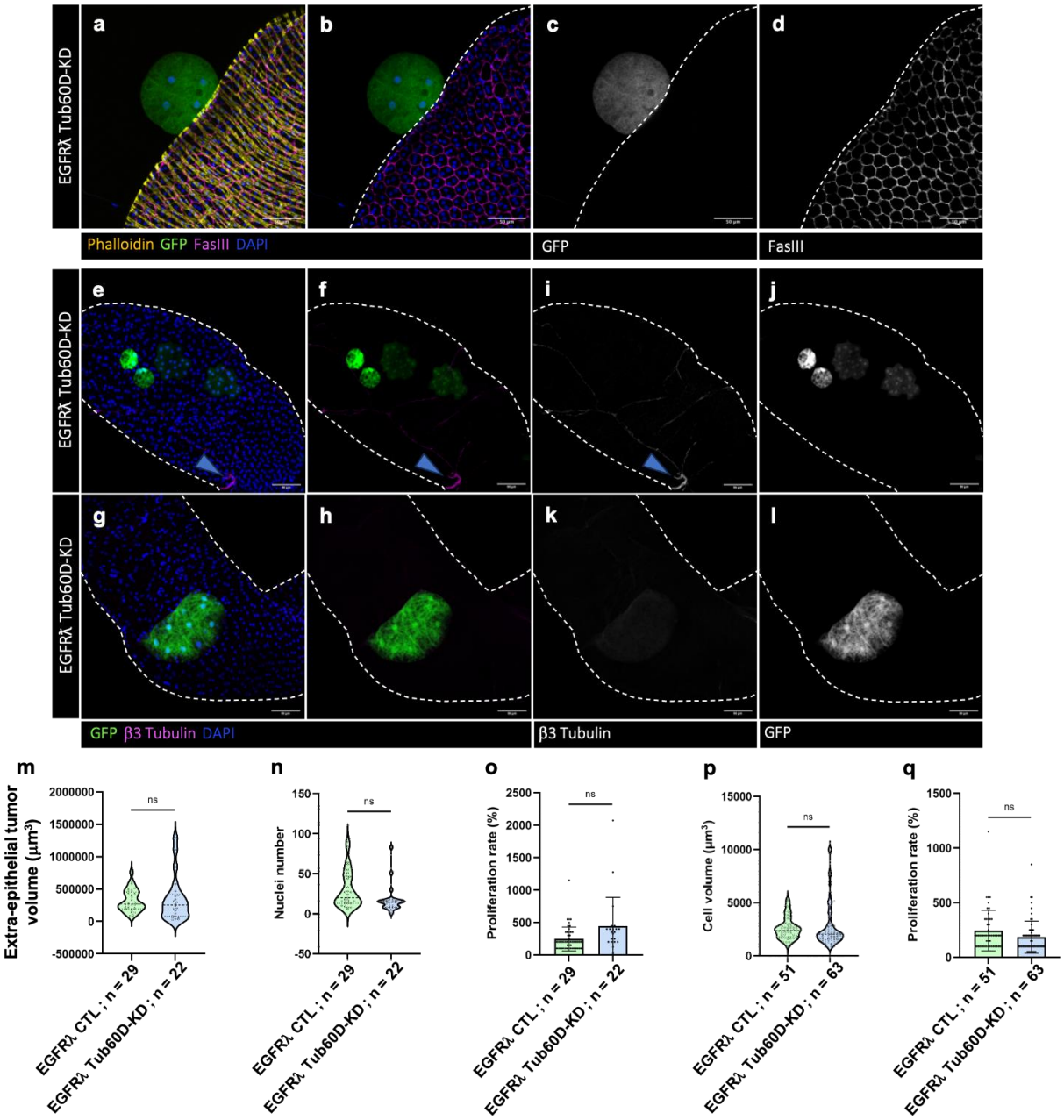

Figure S6- Efficient downregulation of Tub60D has little effect on epithelial tumor cells. (a-d) Co-expression of Tub60D RNAi does not affect the phenotype of extra-epithelial tumors. (e-l) Downregulation of Tub60D efficiently suppresses the accumulation of β3 Tubulin in clonal cells (e-h) and tumor cells (i-l). Remaining staining can be seen in other cell types such as tracheal cells (blue arrowheads in (e-i). (m-q) Characteristics of the different types of tumor cells co-expressing Tub60D RNAi. Extra-epithelial tumors co-expressing Tub60D RNAi display the same size (m), cell number (n) and proliferation rate (o) as EGFRλ CTL tumors. (p-q) Intra-epithelial clones co-expressing Tub60D RNAi are composed of cells of same size (p) which display the same proliferation rate (q) as EGFRλ CTL intra-epithelial clones. Chi^2 test; ns: non significant. Representative images in (a-l) from three or more experiments. Scale bars: 50 µM.

Table S1. Numbers of independent experiments (N) and individuals (n) used in the different experiments.

Figure panel	N = Number of independent experiments	n = total number of individuals
Fig. 1E	3	for respective column : 32, 36, 7, 17, 22, 25
Fig. 2C	EGFRλ CTL: 6; EGFRλ EcR: 8	EGFRλ CTL: 29; EGFRλ EcR: 35
Fig. 2D	for respective column: 4, 3, 30, 4, 3, 36	for respective column: 60, 131, 1144, 217, 123, 1525
Fig. 2E	for respective column: 30, 36	for respective column: 1144, 1525
Fig. 2F	3	for respective column of each panel: 53, 35, 30
Fig. 2G	3	for respective column: 203, 196, 217, 268
Fig. 3A	Left panel: for respective column, 30, 36, 7, 9, 8, 33, 12. Right panel: N = 3 for all columns	Left panel, for respective column: 1144, 1525, 228, 287, 207, 1618, 637. Right panel, for respective column: 203, 217, 52, 126, 62, 252, 167
Fig. 3C	for respective column: 3, 3, 4, 4	For each experimental point, accessory glands for >40 individuals were pooled
Fig. 3F	Left panel: 30, 14; right panel: 3 or more	Left panel: 1576, 354; right panel: 248, 130
Fig. 3G	3 or more	for respective column: 51, 30, 25
Fig. 3H	N = 13 independent cohorts	n = 1140

Bibliography

Anton KA, Kajita M, Narumi R, Fujita Y & Tada M (2018) Src-transformed cells hijack mitosis to extrude from the epithelium. *Nat Commun* 9: 4695

Baumgartner M, Radziwill G, Lorger M, Weiss A & Moelling K (2008) c-Src-mediated epithelial cell migration and invasion regulated by PDZ binding site. *Mol Cell Biol* 28: 642–55

Bogden AE, Haskell PM, LePage DJ, Kelton DE, Cobb WR & Esber HJ (1979) Growth of human tumor xenografts implanted under the renal capsule of normal immunocompetent mice. *Exp Cell Biol* 47: 281–293

Bolis M, Bossi D, Vallerga A, Ceserani V, Cavalli M, Impellizzieri D, Di Rito L, Zoni E, Mosole S, Elia AR, *et al* (2021) Dynamic prostate cancer transcriptome analysis delineates the trajectory to disease progression. *Nat Commun* 12: 7033

Bray F, Ferlay J, Soerjomataram I, Siegel RL, Torre LA & Jemal A (2018) Global cancer statistics 2018: GLOBOCAN estimates of incidence and mortality worldwide for 36 cancers in 185 countries. *CA Cancer J Clin* 68: 394–424

Bruhat A, Tourmente S, Chapel S, Sobrier ML, Couderc JL & Dastugue B (1990) Regulatory elements in the first intron contribute to transcriptional regulation of the beta 3 tubulin gene by 20-hydroxyecdysone in Drosophila Kc cells. *Nucleic Acids Res* 18: 2861–2867

Cai C, Chen S, Ng P, Bubley GJ, Nelson PS, Mostaghel EA, Marck B, Matsumoto AM, Simon NI, Wang H, *et al* (2011) Intratumoral de novo steroid synthesis activates androgen receptor in castration-resistant prostate cancer and is upregulated by treatment with CYP17A1 inhibitors. *Cancer Res* 71: 6503–6513

Carney GE, Wade AA, Sapra R, Goldstein ES & Bender M (1997) DHR3, an ecdysone-inducible early-late gene encoding a Drosophila nuclear receptor, is required for embryogenesis. *Proc Natl Acad Sci U S A* 94: 12024–12029

Chountala M, Vakaloglou KM & Zervas CG (2012) Parvin overexpression uncovers tissue-specific genetic pathways and disrupts F-actin to induce apoptosis in the developing epithelia in Drosophila. *PloS One* 7: e47355

Clarke R, Brünner N, Katzenellenbogen BS, Thompson EW, Norman MJ, Koppi C, Paik S, Lippman ME & Dickson RB (1989) Progression of human breast cancer cells from hormone-dependent to hormone-independent growth both in vitro and in vivo. *Proc Natl Acad Sci U S A* 86: 3649–3653

Dowsett M, Smith IE, Ebbs SR, Dixon JM, Skene A, Griffith C, Boeddinghaus I, Salter J, Detre S, Hills M, *et al* (2006) Proliferation and apoptosis as markers of benefit in neoadjuvant endocrine therapy of breast cancer. *Clin Cancer Res Off J Am Assoc Cancer Res* 12: 1024s–1030s

Dupree JM, Langille GM, Khera M & Lipshultz LI (2014) The safety of testosterone supplementation therapy in prostate cancer. *Nat Rev Urol* 11: 526–530

Ganier O, Schnerch D & Nigg EA (2018) Structural centrosome aberrations sensitize polarized epithelia to basal cell extrusion. *Open Biol* 8: 180044

García-Cruz E, Piqueras M, Ribal MJ, Huguet J, Serapiao R, Peri L, Izquierdo L & Alcaraz A (2012) Low testosterone level predicts prostate cancer in re-biopsy in patients with high grade prostatic intraepithelial neoplasia. *BJU Int* 110: E199-202

Gauhar Z, Sun LV, Hua S, Mason CE, Fuchs F, Li T-R, Boutros M & White KP (2009) Genomic mapping of binding regions for the Ecdysone receptor protein complex. *Genome Res* 19: 1006–1013

Hay CW & McEwan IJ (2012) The impact of point mutations in the human androgen receptor: classification of mutations on the basis of transcriptional activity. *PloS One* 7: e32514

Isaacs JT, Furuya Y & Berges R (1994) The role of androgen in the regulation of programmed cell death/apoptosis in normal and malignant prostatic tissue. *Semin Cancer Biol* 5: 391–400

Kajiwara K, Chen P-K, Abe Y, Okuda S, Kon S, Adachi J, Tomonaga T, Fujita Y & Okada M (2022) Src activation in lipid rafts confers epithelial cells with invasive potential to escape from apical extrusion during cell competition. *Curr Biol CB* 32: 3460-3476.e6

Kuukasjärvi T, Kononen J, Helin H, Holli K & Isola J (1996) Loss of estrogen receptor in recurrent breast cancer is associated with poor response to endocrine therapy. *J Clin Oncol Off J Am Soc Clin Oncol* 14: 2584–2589

Leandro-García LJ, Leskelä S, Landa I, Montero-Conde C, López-Jiménez E, Letón R, Cascón A, Robledo M & Rodríguez-Antona C (2010) Tumoral and tissue-specific expression of the major human beta-tubulin isotypes. *Cytoskelet Hoboken NJ* 67: 214–223

Leiblich A, Marsden L, Gandy C, Corrigan L, Jenkins R, Hamdy F & Wilson C (2012) Bone morphogenetic protein- and mating-dependent secretory cell growth and migration in the Drosophila accessory gland. *Proc Natl Acad Sci* 109: 19292–19297

Locke JA, Guns ES, Lubik AA, Adomat HH, Hendy SC, Wood CA, Ettinger SL, Gleave ME & Nelson CC (2008) Androgen levels increase by intratumoral de novo steroidogenesis during progression of castration-resistant prostate cancer. *Cancer Res* 68: 6407–6415

Lu-Yao GL, Albertsen PC, Moore DF, Shih W, Lin Y, DiPaola RS & Yao S-L (2008) Survival following primary androgen deprivation therapy among men with localized prostate cancer. *JAMA* 300: 173–181

Marshall TW, Lloyd IE, Delalande JM, Näthke I & Rosenblatt J (2011) The tumor suppressor adenomatous polyposis coli controls the direction in which a cell extrudes from an epithelium. *Mol Biol Cell* 22: 3962–3970

Melo S, Guerrero P, Moreira Soares M, Bordin JR, Carneiro F, Carneiro P, Dias MB, Carvalho J, Figueiredo J, Seruca R, *et al* (2023) The ECM and tissue architecture are major determinants of early invasion mediated by E-cadherin dysfunction. *Commun Biol* 6: 1132

Merglen A, Schmidlin F, Fioretta G, Verkooijen HM, Rapiti E, Zanetti R, Miralbell R & Bouchardy C (2007) Short- and long-term mortality with localized prostate cancer. *Arch Intern Med* 167: 1944–1950

Michaud JE, Billups KL & Partin AW (2015) Testosterone and prostate cancer: an evidence-based review of pathogenesis and oncologic risk. *Ther Adv Urol* 7: 378–387

Nami B & Wang Z (2018) Genetics and Expression Profile of the Tubulin Gene Superfamily in Breast Cancer Subtypes and Its Relation to Taxane Resistance. *Cancers* 10

Petryk A, Warren JT, Marqués G, Jarcho MP, Gilbert LI, Kahler J, Parvy J-P, Li Y, Dauphin-Villemant C & O'Connor MB (2003) Shade is the Drosophila P450 enzyme that mediates the hydroxylation of ecdysone to the steroid insect molting hormone 20-hydroxyecdysone. *Proc Natl Acad Sci U S A* 100: 13773–13778

Rambur A, Lours-Calet C, Beaudoin C, Buñay J, Vialat M, Mirouse V, Trousson A, Renaud Y, Lobaccaro J-MA, Baron S, *et al* (2020) Sequential Ras/MAPK and PI3K/AKT/mTOR pathways recruitment drives basal extrusion in the prostate-like gland of Drosophila. *Nat Commun* 11: 2300

Sekar A, Leiblich A, Wainwright SM, Mendes CC, Sarma D, Hellberg JEEU, Gandy C, Goberdhan DCI, Hamdy FC & Wilson C (2023) Rbf/E2F1 control growth and endoreplication via steroid-independent Ecdysone Receptor signalling in Drosophila prostate-like secondary cells. *PLoS Genet* 19: e1010815

Sharma V, Pandey AK, Kumar A, Misra S, Gupta HPK, Gupta S, Singh A, Buehner NA & Ravi Ram K (2017) Functional male accessory glands and fertility in Drosophila require novel ecdysone receptor. *PLoS Genet* 13: e1006788

Shen J, Lu J, Sui L, Wang D, Yin M, Hoffmann I, Legler A & Pflugfelder GO (2014) The orthologous Tbx transcription factors Omb and TBX2 induce epithelial cell migration and extrusion in vivo without involvement of matrix metalloproteinases. *Oncotarget* 5: 11998–12015

Shirai T, Sekai M, Kozawa K, Sato N, Tanimura N, Kon S, Matsumoto T, Murakami T, Ito S, Tilston-Lunel A, *et al* (2022) Basal extrusion of single-oncogenic mutant cells induces dome-like structures with altered microenvironments. *Cancer Sci* 113: 3710–3721

Slaidina M, Delanoue R, Gronke S, Partridge L & Léopold P (2009) A Drosophila insulin-like peptide promotes growth during nonfeeding states. *Dev Cell* 17: 874–884

Slattum G, McGee KM & Rosenblatt J (2009) P115 RhoGEF and microtubules decide the direction apoptotic cells extrude from an epithelium. *J Cell Biol* 186: 693–702

Ventrella R, Kim SK, Sheridan J, Grata A, Bresteau E, Hassan OA, Suva EE, Walentek P & Mitchell BJ (2023) Bidirectional multiciliated cell extrusion is controlled by Notch-driven basal extrusion and Piezo1-driven apical extrusion. *Dev Camb Engl* 150: dev201612

Vialat M, Baabdaty E, Trousson A, Kocer A, Lobaccaro J-MA, Baron S, Morel L & de Joussineau C (2024) Cholesterol Dietary Intake and Tumor Cell Homeostasis Drive Early Epithelial Tumorigenesis: A Potential Modelization of Early Prostate Tumorigenesis. *Cancers* 16

Villeneuve C, Lagoutte E, de Plater L, Mathieu S, Manneville J-B, Maître J-L, Chavrier P & Rossé C (2019) aPKCi triggers basal extrusion of luminal mammary epithelial cells by tuning contractility and vinculin localization at cell junctions. *Proc Natl Acad Sci U S A* 116: 24108–24114

Wilson C, Leiblich A, Goberdhan DCI & Hamdy F (2017) The Drosophila Accessory Gland as a Model for Prostate Cancer and Other Pathologies. In *Current topics in developmental biology* pp 339–375.

Wu HC, Hsieh JT, Gleave ME, Brown NM, Pathak S & Chung LW (1994) Derivation of androgen-independent human LNCaP prostatic cancer cell sublines: role of bone stromal cells. *Int J Cancer* 57: 406–412

Xue L & Noll M (2002) Dual role of the Pax gene paired in accessory gland development of Drosophila. *Dev Camb Engl* 129: 339–46

Zoeller JJ, Bronson RT, Selfors LM, Mills GB & Brugge JS (2017) Niche-localized tumor cells are protected from HER2-targeted therapy via upregulation of an anti-apoptotic program in vivo. *NPJ Breast Cancer* 3: 18